

## A STUDY OF MICROSTRUCTURE AND MECHANICAL PROPERTIES OF THICK WELDED JOINTS OF A Cr – Mo STEEL

I Kon Lee<sup>1</sup> and Yi Cheng Chien<sup>2</sup>

Translated from *Metallovedenie i Termicheskaya Obrabotka Metallov*, No. 3, pp. 53 – 59, March, 2015.

The effect of stress-relieving tempering on the mechanical properties of a welded joint of a high-strength low-alloy steel SAE 4130 (0.3% C – 1% Cr – 0.25% Mo) obtained by multipass arc welding with nonconsumable electrode is studied. The steel is quenched and tempered before the welding. An optimum tempering mode providing a good combination of the characteristics of strength, ductility and toughness of the welded joint is suggested.

**Key words:** high-strength low-alloy steels, welding with nonconsumable electrode, mechanical properties.

### INTRODUCTION

Steel SAE 4130 (0.3% C + 1% Cr + 0.3% Mo) is a high-temperature low-alloy grade, where a martensitic structure forms easily due to the presence of chromium and molybdenum. The hardenability of SAE 4130 exceeds that of carbon steels with equivalent carbon content [1 – 4]. The AMS-6370N, AMS-2632 and AMS-2630B Standards stipulate the hardness level of SAE 4130 after a heat treatment in sections larger than 12.7 mm (0.5 inch) [4 – 7].

In the case of gas tungsten arc welding (GTAW) the welded material is affected by the welding thermal cycle in the heat-affected zone (HAZ) [7, 8]. In multipass welding the zone affected by reheating from the next pass is termed reheated zone. The weld zone not affected by reheating is known as that of primary fusion. The residual stresses arising

in the welding process lower the strength and other mechanical properties of the steel [9 – 12]. The effect of residual stresses can be reduced by preheating, temperature control between the passes, post welding heat treatment (PWHT), and other measures [13, 14].

The aim of the present work was to determine the efficiency of stress relieving after thermal refining and multipass welding of steel SAE 4130 on the basis of results of determination of the microstructure and mechanical properties.

### METHODS OF STUDY

The chemical composition of rolled plates from steel SAE 4130 (Table 1) was determined by spectroscopy according to AMS 6370M [4]. A plate from steel SAE 4130 was rolled for a thickness of 16.5 mm and subjected to total annealing and thermal refining (Table 2). Then we performed multilayer welding with nonconsumable electrode and tempering for relieving the stresses. The welding parameters are given in Table 3.

It should be noted that the welding electrode (rod) met the requirements of AMS-6557C [15]. The first welding ope-

<sup>1</sup> Department of Materials Science and Engineering, Da-Yeh University, Changhua, Taiwan, Republic of China (e-mail: iklee@mail.dyu.edu.tw).

<sup>2</sup> Department of Mechanical and Automation Engineering, Da-Yeh University, Changhua, Taiwan, Republic of China.

**TABLE 1.** Chemical Composition of Steel SAE 4130

Steel SAE 4130	Content of elements, wt.%						
	C	Cr	Mo	Mn	Si	S	P
Specified by AMS 6370M	0.28 – 0.33	0.80 – 1.10	0.15 – 0.25	0.40 – 0.60	0.20 – 0.35	< 0.040	< 0.035
Used actually	0.32	0.84	0.20	0.41	0.32	0.007	0.007

**TABLE 2.** Modes of Heat Treatment of Plates from Steel SAE 4130

Heat treatment	Mode
Total annealing (A)	870°C, 40 min, cooling with the furnace
Thermal refining (TR):	
quenching (Q)	860°C, 90 min, oil quenching
tempering (T)	500°C, 70 min, air cooling
Stress relieving (SR)	550°C, 2 h, cooling with the furnace

**TABLE 3.** Parameters of Multipass Gas Tungsten Arc Welding (GTAW)

Welding variant	$I$ , A	$U$ , V	$v$ , mm/min	Electrode	$t_i$ , °C
1	160	12	76.2	AMS 6457C	> 50 (heating)
2	260	13	889.0		> 250

**Notations:**  $I$ ) current;  $U$ ) voltage;  $v$ ) speed of welding;  $t_i$ ) inter-pass temperature.

ration was made manually so as to penetrate to the root of the weld. All the other welding stages were performed automatically in the GTAW mode.

We cut transverse specimens for analyzing the microstructure of the welded joints and measuring the Vickers hardness with the help of a Vickers microhardness tester at a load of 2 N with a hold of 10 sec. The hardness was measured every 0.1 mm in the base metal on both sides of the weld and in the weld itself. The specimens were immersed into a solution of 1.5 ml  $\text{HNO}_3$  + 100 ml  $\text{C}_2\text{H}_5\text{OH}$  to etch the surfaces. The metal of the weld, of the heat-affected zone, and of the base was studied with the help of optical, scanning, and transmission electron microscopy. The scanning electron microscope was used for an energy dispersive chemical analysis.

The specimens for tensile tests matched the ASTM E8M Standard; the tests were performed according to ASTM B557.

The speed of the deformation was 0.5 mm/min. The specimens for the impact toughness tests had a size of  $10 \times 10 \times 55$  mm according to ASTM E23.

## RESULTS AND DISCUSSION

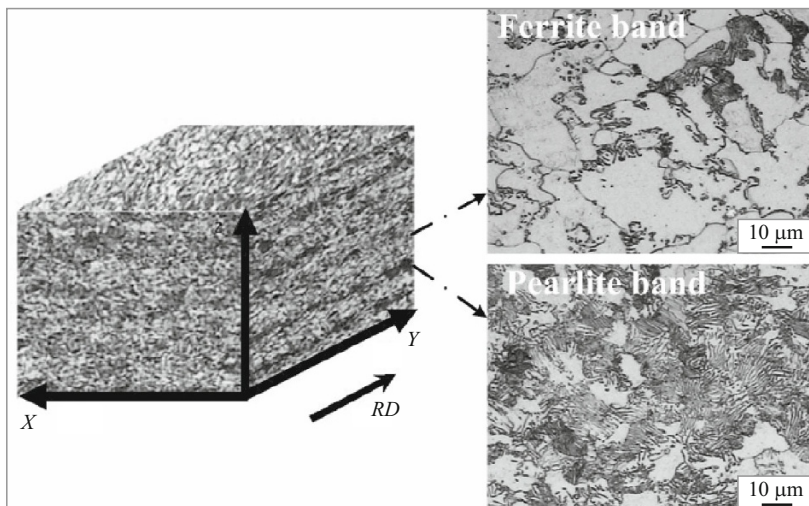
### Microhardness and Microstructure of Welded Joint

Figure 1 presents the microstructure of annealed steel SAE 4130. It can be seen that the structure has a stripped pattern oriented over the rolling axis ( $Y$ ) [16, 17]. Such a pattern is connected with segregation of phosphorus and molybdenum [18].

The process of multipass gas tungsten arc welding (GTAW) with nonconsumable electrode is described in the ASM Handbook [19]. The welded joint was classified in accordance with the succession of passes as follows: the last-layer weld (LW), the reciprocal second-layer weld (R2W), and the reciprocal third-layer weld (R3W). The microstructure of the heat-affected zone is commonly divided into the following regions [20]: a grain growth zone, a recrystallized zone, a zone of partial transformation, a tempered zone, and a zone of unaffected base material. The structural transformations under continuous cooling (CCT diagrams) for the steel are described in [21].

After quenching, steel SAE 4130 should have a martensitic structure. However, in a massive plate the structure transforms from a martensitic one to a mixture of bainite and retained austenite in the direction from the surface to the core. After tempering at 500°C the surface layers of the steel consist primarily of tempered martensite and a ferrite-carbide mixture. In the center of a massive specimen the structure is stripped due to segregations (Fig. 2).

Figure 3 presents the curves of the variation of microhardness over the thickness of a welded joint after refining and multipass welding with subsequent heat treatment for relieving stresses and without the later (variants 1 and 2, respectively). Two minimums of microhardness are observable



**Fig. 1.** Triaxial diagram of the structure of annealed steel SAE 4130 with respect to the rolling direction ( $RD$ ) (optical microscopy).

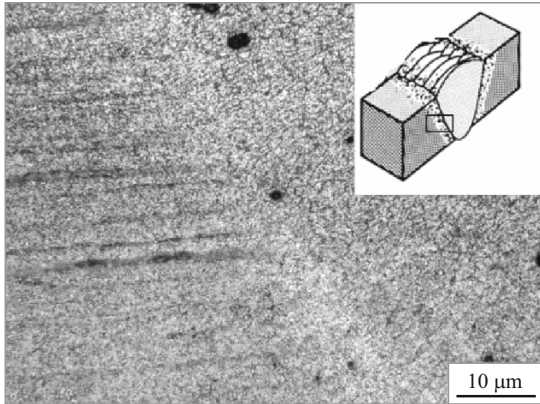


**Fig. 2.** Structure of a welded joint of a 16.5 mm-thick plate of steel SAE 4130 (optical microscopy).

between the last and second and the second and third passes for both variants. Figure 4a presents a diagram of the multipass welding. Figure 4b presents the structure of the last weld layer in the zone of primary fusion, which has been cooled from liquid state to solid state without an external heat effect. Figure 4d presents the structure of the fusion zone in the second weld layer; Fig. 4c presents the structure of the zone between the last and second layers. Since this region has been affected by the heat of the last pass, its structure is coarser, which agrees with the minimum of microhardness in this zone.

Minimum values of microhardness occur in the heat-affected zones on both sides of the welded joint. Since the peak temperatures of the welding thermal cycle exceed point  $A_1$  in the zones of grain growth, recrystallization, and partial transformation, the final structures are determined by the continuous cooling transformation diagram plotted in [21]. The

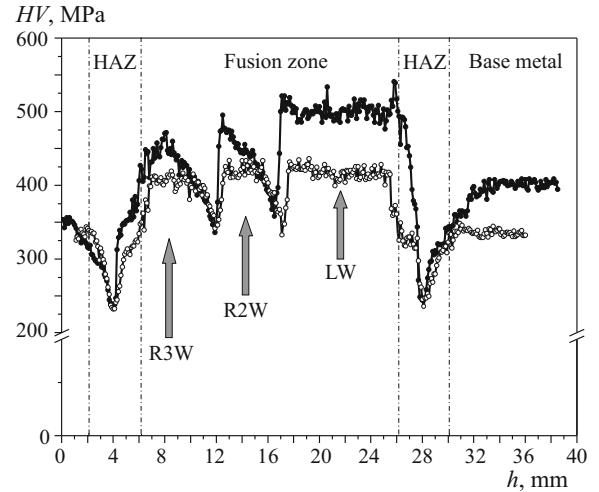


**Fig. 3.** Variation of microhardness over cross section of a welded joint from steel SAE 4130 ( $h$  is the distance over the section):  $\blacklozenge$  thermal refining + welding (ASTW);  $\diamond$  thermal refining + welding + tempering for stress relieving (ASTWR); LW, R2W, R3W) last weld layer, reciprocal second weld layer, and reciprocal third weld layer.

microstructure of individual regions of the heat-affected zone is presented in Fig. 5. We observe transition from the structure of coarse martensite with bainite and retained austenite (Fig. 5a) to a mixture of ferrite and cementite in the tempered zone (Fig. 5b, c, and d).

As a rule, thermal refining and precision mechanical treatment precede welding of chromium-molybdenum steels. Only a heat treatment is required for relieving stresses after the welding. When the residual thermal stresses are relieved, the hardness of the weld is somewhat lowered. It can be seen from Fig. 3 that the hardness minimums after relieving of the

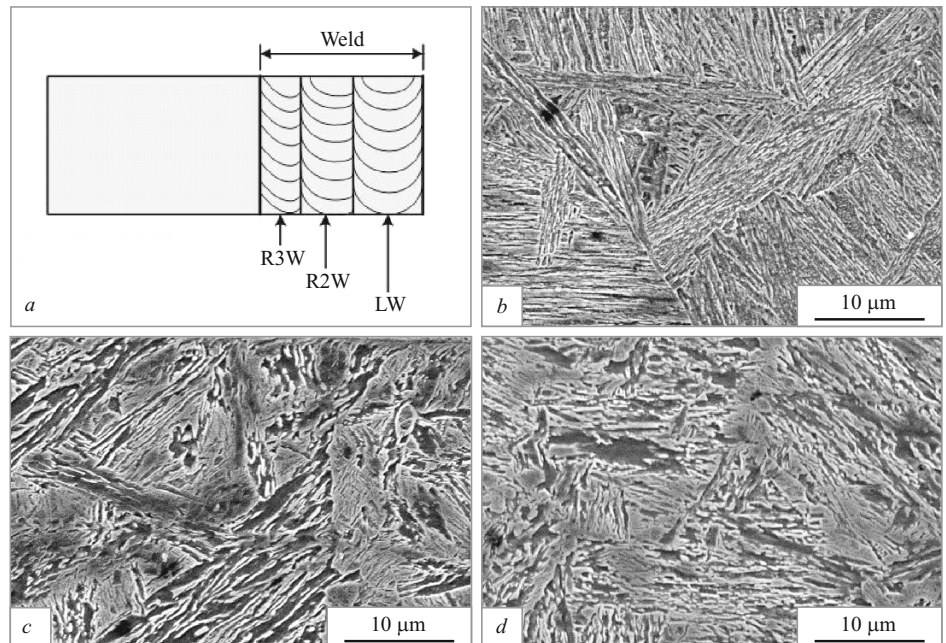


**Fig. 4.** Microstructure of a weld region formed by multipass GTAW of steel SAE 4130 after thermal refinement without heat treatment for relieving stresses (scanning electron microscopy): a) welding diagram; b) last weld layer; c) boundary between the last and second weld layers; d) second weld layer.

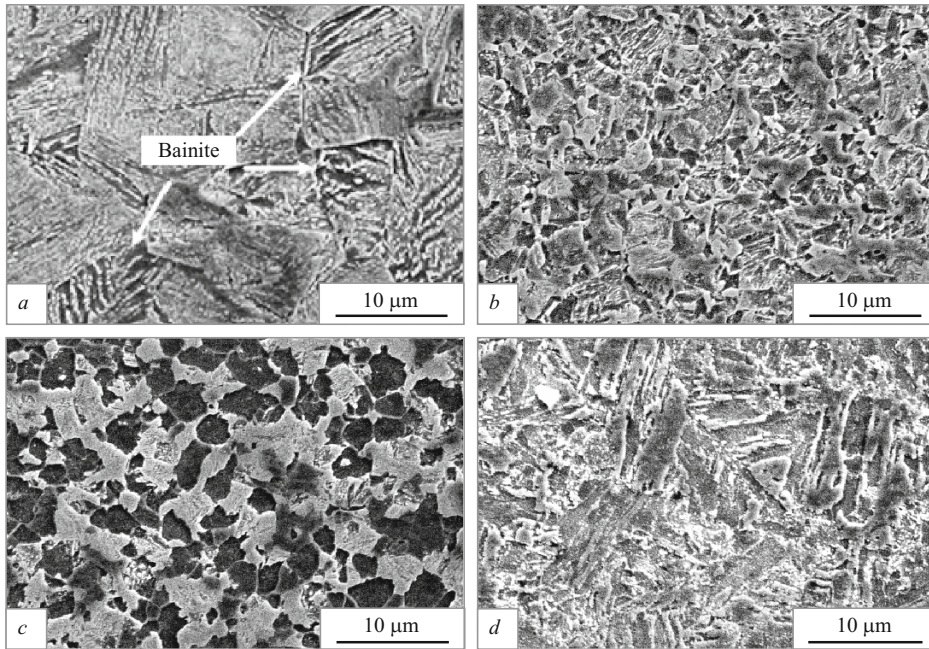


**Fig. 5.** Microstructure of the HAZ of a welded joint from steel SAE 4130 after thermal refining (scanning electron microscopy): *a*) grain growth region; *b*) region of recrystallization; *c*) region of partial transformation; *d*) tempered region.

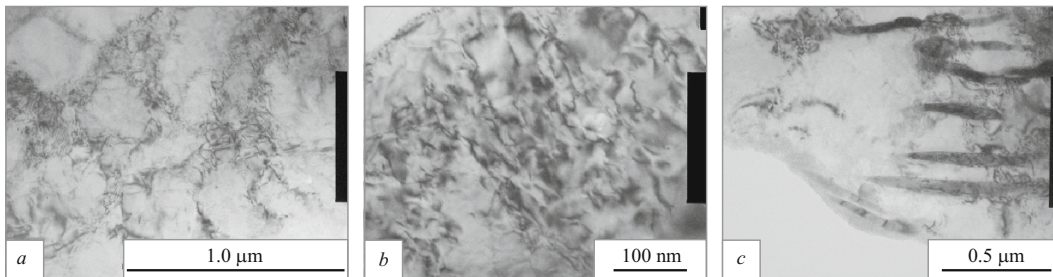


**Fig. 6.** Microstructure of a welded joint from steel SAE 4130 after thermal refining, welding and stress-relieving heat treatment (transmission electron microscopy): *a*) base metal; *b*) heat-affected zone; *c*) weld.

stresses do not disappear and do not change their position. The microstructure of different zones also remains unchanged after relieving the stresses except for the decomposition of the retained austenite into ferrite and cementite. By

the data of the transmission electron microscopy stress relieving does not produce segregations either in the heat-affected zone or in the base metal, while the metal of the weld acquires lenticular segregations (Fig. 6).

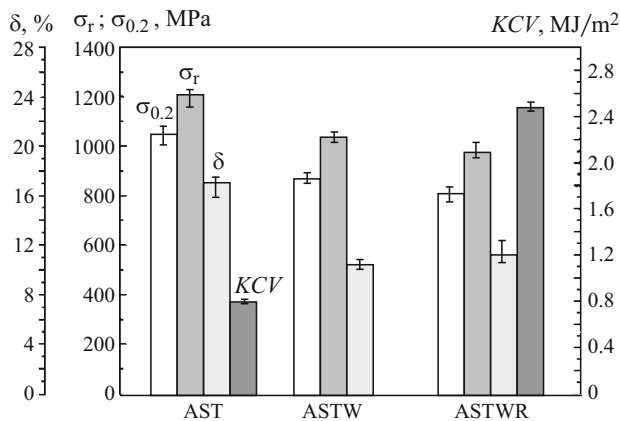


**Fig. 7.** Mechanical properties of welded joints of steel SAE 4130: AST) annealing + thermal refining; ASTW) annealing + refining + welding; ASTWR) annealing + refining + welding + stress-relieving tempering.

**Tensile Tests**

According to the ASM Handbook [22], standard steel SAE 4130 in tempered condition (500°C, 70 min, air cooling) has the following mechanical characteristics:  $\sigma_r = 1100$  MPa,  $\sigma_{0.2} = 906$  MPa,  $\delta = 18.8\%$ . Analyzing the data of Fig. 7 we will see that the mechanical properties of SAE 4130 after annealing, thermal refining and tempering match the standardized values, though the elongation is somewhat lower. On the contrary, the welded joint not subjected to a stress relieving treatment has a rupture strength of 86% and an elongation of 61% of the corresponding pre-welding values. Tempering for stress relieving reduces  $\sigma_r$  to 81% of the initial value and raises  $\delta$  to 66%.

Macro- and micro-fractographs of the studied specimens are presented in Fig. 8. The macro-fractographs (Fig. 8*a – c*) show that the welded joint fails over the heat-affected zone near the interface with the weld, which matches the hardness

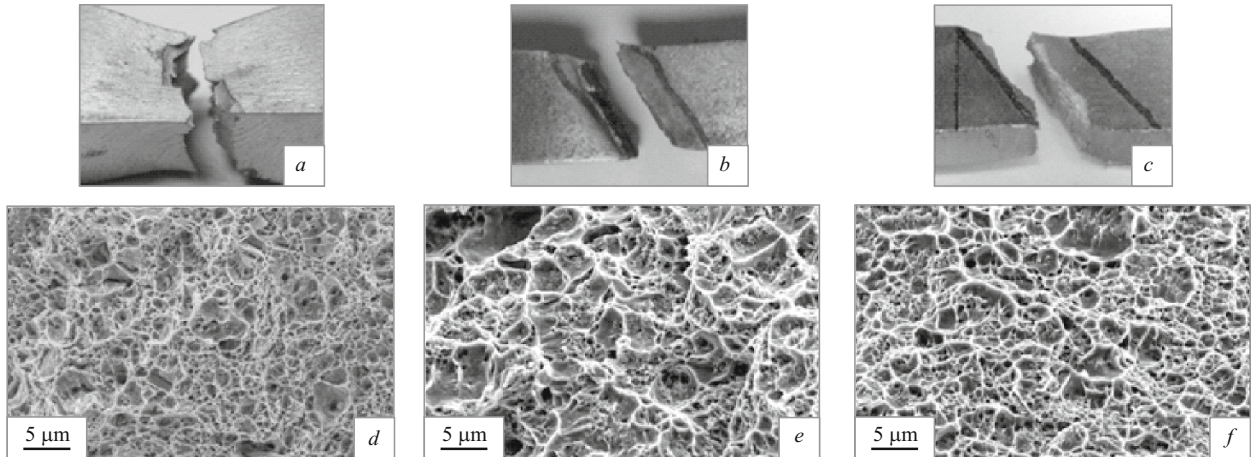


**Fig. 8.** Appearance (*a – c*) and fractographs of specimens of steel SAE 4130 after testing for impact strength. Prior to the tests, the specimens have been subjected to: *a, d*) refining (AST); *b, e*) refining + welding (ASTW); *c, f*) refining + welding + stress relieving (ASTWR).

minimum (Fig. 3). In the condition prior to the welding (after thermal refining and tempering) the neck is the most prominent.

The micro-fractograph in Fig. 8*d* shows that the fracture surface before the welding corresponds to the most ductile fracture mechanism with dimple pattern. After the welding, the dimple fracture is coarser (Fig. 8*e*). The stress-relieving tempering does not introduce significant changes into the fracture behavior as compared to the state after the welding (Fig. 8*f*).

**Tests for Impact Toughness**

We notched impact specimens over the interface of the first-layer weld and the heat-affected zone. The data of Fig. 7 show that after the welding and stress-relieving tempering

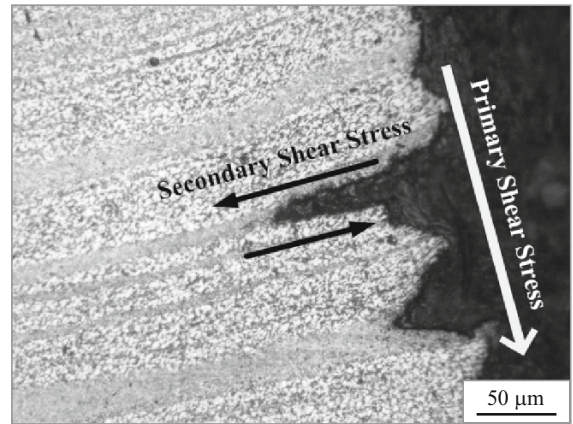


**Fig. 9.** Structure of a cross section of an impact specimen after welding, stress-relieving tempering, and impact testing until failure.

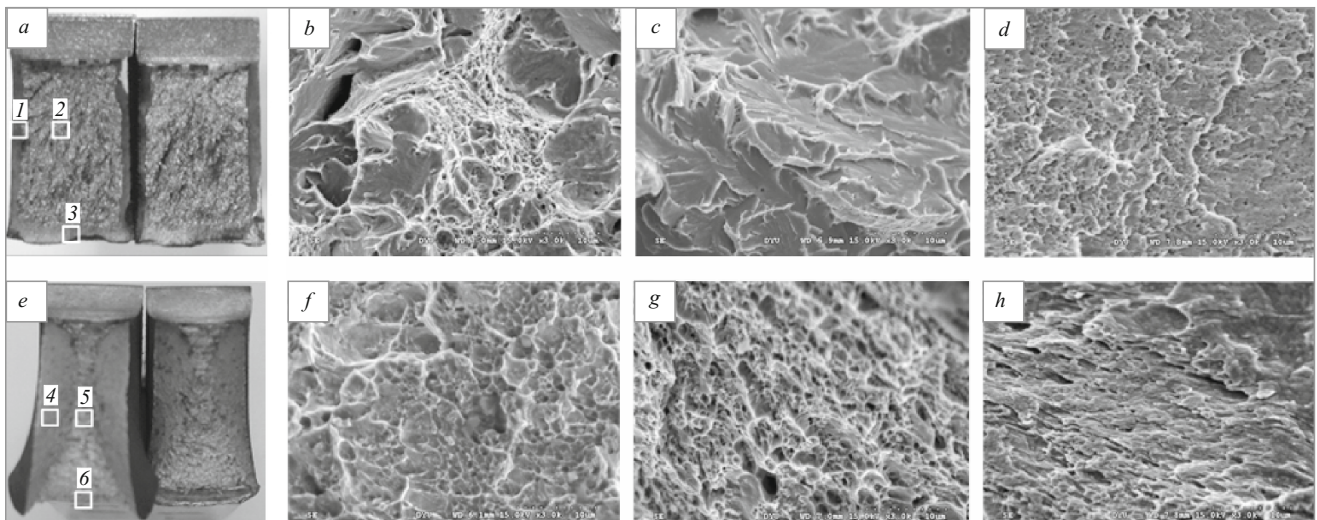


**Fig. 10.** Fractographs of specimens of steel SAE 4130 after testing for impact strength. The treatment before the tests: *a – d*) annealing + thermal refining (AST); *e – h*) annealing + refining + welding + stress-relieving tempering (ASTWR); *a, e*) macro-fractographs; *b, c, d*) microfractures in regions 1, 2, 3, respectively; *f, g, h*) microfractures in regions 4, 5, 6, respectively.

the impact toughness increased by about a factor of 3 as compared to the pre-welding value. It can be seen from Fig. 9 that the welded joint fractured from the tip of the notch in the direction of the principal shear stress. However, cracks formed due to the difference in the mechanical properties of ferrite and bainite are observable almost perpendicularly to the principal direction over the segregation bands.

Figure 10 presents fractographs of impact specimens in different states. It can be seen that the macro- and micro-fractographs agree well with the results of the impact tests. The fracture surfaces of the impact specimens in the pre-welding condition are represented by a mixture of dimple fracture and cleavages (Fig. 10a – d). The fracture in region 2 consists primarily of quasi-cleavage zones; in region 3 it corresponds to a large tearing crack. The micro-fractographs of the specimens after welding and stress relieving have a finer dimple morphology (Fig. 10e – h). In the end of the specimen (region 6) we observe a tearing crack. On the whole, this specimen exhibits a more ductile fracture behavior.

## CONCLUSIONS

1. Stress-relieving tempering at 550°C after multipass arc welding of steel SAE 4130 (0.3% C – 1% Cr – 0.25% Mo) provides in the welded joint a rupture strength equal to 81% and an elongation equal to 66% of the initial values of these characteristics (after quenching with high tempering).

2. Stress-relieving tempering at 550°C after multipass arc welding raises the impact toughness of the heat-affected zone of the weld by about a factor of 3 with respect to the impact toughness of the steel after thermal refining.

3. Impact specimens fail over the heat-affected zone, which agrees with the distribution of microhardness in the welded joint between the weld material and the heat-affected zone.

## REFERENCES

1. W. M. Carrison, "Ultrahigh-strength steels for aerospace applications," *J. Mater.*, **42**(5), 20 – 24 (1990).
2. K. M. Zwilsky, "Classification and designation of carbon and low-alloy steels," in: *Metal Handbook, Properties and Selection: Irons, Steel, and High-Performance Alloys*, Materials Park, OH, ASM International (1990), Vol. 1, pp. 140 – 194.
3. M. C. Tsai, *Microstructural Evolution of Simulated Heat-Affected Zone in Cr – Mo Alloy Steels and Phase Transformations in an AISI 410 Stainless Steel*, Author's Abstract of Doctoral's Thesis, National Taiwan University, Taiwan (2002).
4. *AMS-6370M, Steel Bars, Forgings, and Rings, 0.95Cr – 0.20Mo (0.28 – 0.33C)*, Society of Automotive Engineers, USA (2006).
5. *AMS-2632. Ultrasonic, of Thin Materials, 0.5 inch (12.7 mm) and under in Cross-Sectional Thickness*, Society of Automotive Engineers, USA (1995).
6. *AMS-2630B. Ultrasonic, Product over 0.5 inch (12.7 mm) Thick*, Society of Automotive Engineers, USA (1995).
7. C. C. Hsieh, T. C. Chang, D. Y. Lin, et al., "Precipitation behavior of  $\sigma$  phase in fusion zone of dissimilar stainless steels welds during multi-pass GTAW process," *Met. Mater. Int.*, **13**, 411 – 416 (2007).
8. D. L. Olson, "Solid-state transformations in weldments," in: *Metal Handbook. Welding, Brazing, and Soldering*, Materials Park, OH, ASM International (1997), Vol. 1.6, pp. 70 – 87.
9. S. Murugan, S. K. Rai, P. V. Kumar, et al., "Temperature distribution and residual stresses due to multipass welding in type 304 stainless steel and low carbon steel weld pads," *Int. J. Pressure Vessels Piping*, **78**(4), 307 – 317 (2001).
10. S. Murugan, P. V. Kumar, B. Raj, and M. S. C. Bose, "Temperature distribution during multipass welding of plates," *Int. J. Pressure Vessels Piping*, **75**(12), 891 – 905 (1998).
11. S. K. Albert, T. P. S. Gill, A. K. Tyagi, et al., "Soft zone formation in dissimilar welds between two Cr – Mo steels," *Welding J.*, **76**(3), 135s – 142s (1997).
12. J. R. Cho, B. Y. Lee, Y. H. Moon, and C. J. Van Tyne, "Investigation of residual stress and post weld heat treatment of multipass welds by finite element method and experiments," *J. Mater. Proc. Technol.*, **155 – 156**, 1690 – 1695 (2004).
13. C. C. Huang, Y. C. Pan, and T. H. Chuang, "Effect of post-weld heat treatments on the residual stress and mechanical properties of electron beam welded SAE 4130 steel plates," *J. Mater. Eng. Perform.*, **6**(1), 61 – 68 (1997).
14. I. K. Lee, C. L. Chung, Y. Y. Lee, and Y. T. Chien, "Study of thermal refining on mechanical properties of annealed SAE 4130 by multilayer GTAW," *J. Iron Steel Res. Int.*, **19**(7), 71 – 78 (2012).
15. *Steel, Welding Wire 0.95Cr – 0.20Mo (0.28 – 0.33C) Vacuum Melted. Environmental Controlled Packaging SAE 4130*, Society of Automotive Engineers, AMS 6457C, USA (2001).
16. G. Krauss, "Solidification, segregation, and banding in alloy steels," *Metall. Mater. Trans. B*, **34**, 781 – 792 (2003).
17. S. N. Prasad Saxena, S. Goswami, J. Subudhi, and S. K. Chaudhuri, "Influence of austempering parameters on the microstructure and tensile properties of a medium carbon-manganese steel," *Mater. Sci. Eng. A*, **431**, 53 – 58 (2006).
18. M. R. Barnett, R. Balasubramaniam, Vinod Kumar, and Colin MacRae, "Correlation between microstructure and phosphorus segregation in a hypereutectoid Wootz steel," *J. Mater. Sci.*, **44**(9), 2192 – 2197 (2009).
19. C. B. Dallam and B. K. Damkroger, "Characterization of welds," in: *Metal Handbook, Welding, Brazing and Soldering*, ASM Int. (1997), Vol. 6, pp. 97 – 106.
20. W. S. Lee and T. T. Su, "Mechanical properties and microstructural features of AISI 4340 high-strength alloy steel under quenched and tempered conditions," *J. Mater. Proc. Technol.*, **87**, 198 – 206 (1999).
21. S. M. Copley, "Quenching of steel," in: *Metal Handbook, Heat Treating*, Materials Park, OH, ASM Int. (1991), Vol. 4, pp. 84 – 87.
22. T. V. Philip, "Heat treating of ultrahigh-strength steels," in: *Metal Handbook, Heat Treating*, ASM Int. (1981), Vol. 4, pp. 119 – 129.